

# A Novel High Efficiency High Step-up Interleaved Converter with Voltage Multiplier Circuit for a PV System

D.Byragi Naidu<sup>1</sup>, D.Vijaya kumar<sup>2</sup>, Bibhuti bhusan rath<sup>3</sup>

<sup>1</sup>P.G student, Dept. of EEE, AITAM Engineering College, AP, India, duppatlaeee@gmail.com

**Abstract-** A high step-up converter is proposed for a photovoltaic system. A voltage multiplier used here provides high voltage gain without extreme duty cycle. The voltage multiplier is composed of a conventional boost converter and coupled inductors. An extra conventional boost converter is integrated into the first phase to achieve a considerably higher voltage conversion ratio. The two-phase configuration not only reduces the current stress through each power switch, but also constrains the input current ripple, which decreases the conduction losses of metal-oxide-semiconductor field-effect transistors (MOSFETs). It also functions as a clamp circuit which alleviates the voltage spikes across the power switches. So, the low-voltage-rated MOSFETs can be adopted for reductions of conduction losses and cost. Efficiency improves because the energy stored in leakage inductances is recycled to the output terminal.

**Keywords-** Boost-Fly back converter, High step-up, photovoltaic system, Voltage multiplier module.

## I. INTRODUCTION

Renewable sources of energy are increasingly valued worldwide because of energy shortage and environmental contamination. Renewable energy systems generate low voltage output and thus, high step-up dc/dc converters are widely employed in many renewable energy applications, including fuel cells, wind power, and photovoltaic systems are expected to play an important role in future energy production. Such system transform light energy into electrical energy, and convert low voltage into high voltage via a step-up converter, which can convert energy into electricity using a grid-by-grid inverter or store energy into a battery set. Figure 1 shows a typical photovoltaic system that consists of a solar module, a high step up converter, a charge-discharge controller, a battery set, and an inverter.

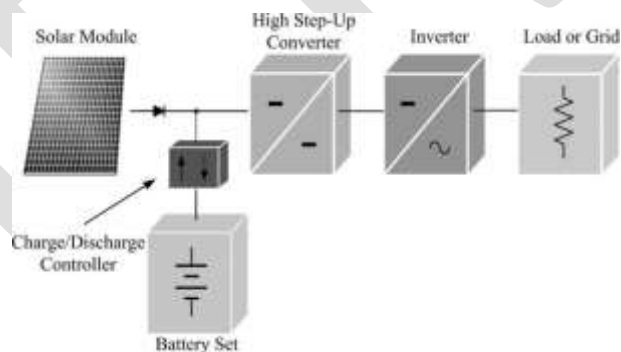


Figure 1: Typical Photovoltaic System

Conventional step-up converters, such as the boost converter and flyback converter, cannot achieve a high step-up conversion with high efficiency because of the resistances of elements or leakage inductance. Thus, a modified boost-flyback converter was proposed. Modifying a boost-fly back converter, shown in Figure 2(a) is one of the simple approaches step-up gain and the gain is realized via a coupled inductor. The performance of the converter is similar to an active-clamped flyback converter; thus, the leakage energy is recovered to the output terminal. An interleaved boost converter with a voltage-lift capacitor shown in Figure 2(b) is highly similar to the conventional interleaved type. It obtains extra voltage gain through the voltage-lift capacitor, and reduces the input current ripple, which is suitable for power factor correction (PFC) and high-power applications.

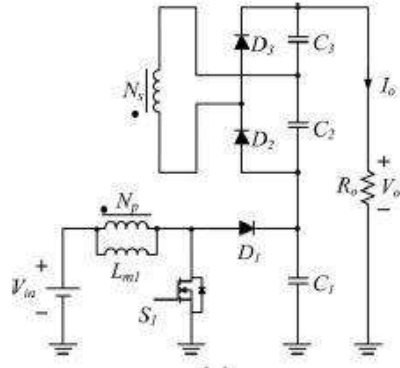


Figure 2(a): Modified Boost Flyback Converter

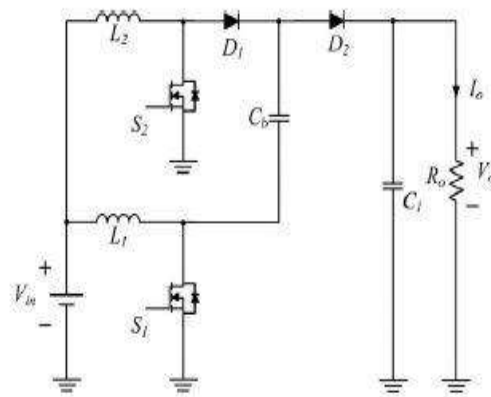


Figure 2(b): Interleaved Boost Converter with a Voltage-lift Capacitor Structure

## II. PROPOSED TOPOLOGY

In this paper, an asymmetrical interleaved high step-up converter that combines the advantages of the aforementioned converters is proposed, which combined the advantages of both. In the voltage multiplier module of the proposed converter, the turns ratio of coupled inductors can be designed to extend voltage gain, and a voltage-lift capacitor offers an extra voltage conversion ratio. The advantages of the proposed converter are as follows:

- 1) The converter is characterized by a low input current ripple and low conduction losses, making it suitable for high power applications;
- 2) The converter achieves the high step-up voltage gain that renewable energy systems require;
- 3) Leakage energy is recycled and sent to the output terminal, and alleviates large voltage spikes on the main switch;
- 4) The main switch voltage stress of the converter is substantially lower than of the output voltage.
- 5) Low cost and high efficiency are achieved.

### A. Circuit Description

The proposed high step-up converter with voltage multiplier module is shown in Figure 3(a). A conventional boost converter and two coupled inductors are located in the voltage multiplier module, which is stacked on a boost converter to form an asymmetrical interleaved structure. Primary windings of the coupled inductors with  $N_p$  turns are employed to decrease input current ripple, and secondary windings of the coupled inductors with  $N_s$  turns are connected in series to extend voltage gain. The turns ratios of the coupled inductors are the same. The coupling references of the inductors are denoted by “.” and “\*”.

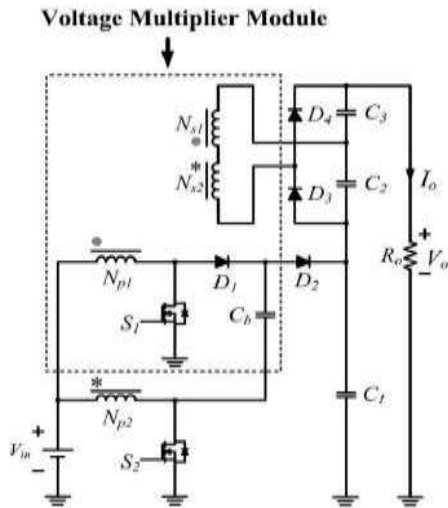


**Figure 3(a): Proposed High Step-up Converter with a Voltage Multiplier Module**

The equivalent circuit of the proposed converter is shown in Figure 3(b), where  $L_{m1}$  and  $L_{m2}$  are the magnetizing inductors,  $L_{k1}$  and  $L_{k2}$  represent the leakage inductors,  $S_1$  and  $S_2$  denote the power switches,  $C_b$  is the voltage-lift capacitor, and  $n$  is defined as a turns ratio  $N_s/N_p$ .

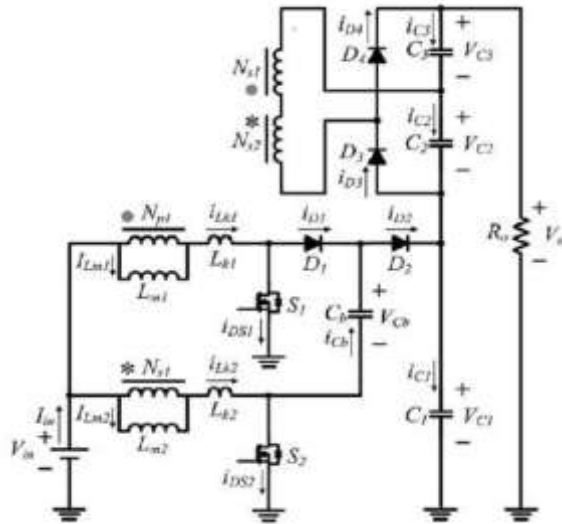


**Figure 3(b): Equivalent Circuit**

### III. MODAL ANALYSIS

The proposed converter operates in continuous conduction mode (CCM), and the duty cycles of the power switches during steady operation are interleaved with a  $180^\circ$  phase shift and the duty cycles are greater than 0.5. The key steady waveforms in one switching period of the proposed converter contain six modes.

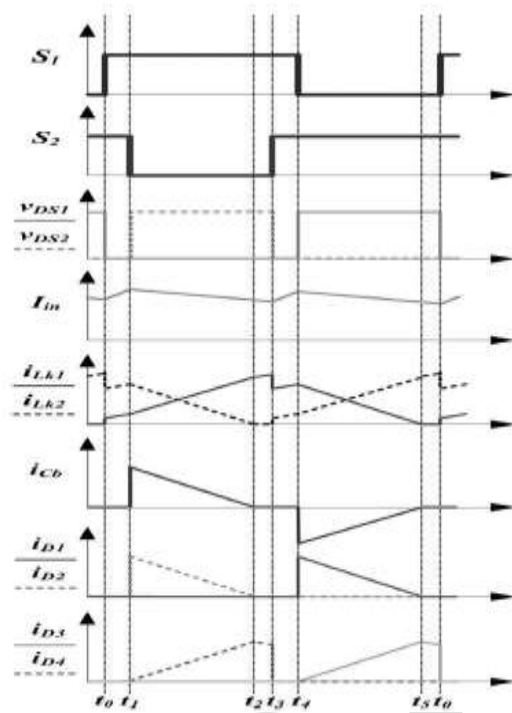


**Figure 4: Steady Waveforms of the Proposed Converter**

**Mode 1** [ $t_0, t_1$ ]: At  $t = t_0$ , the power switches  $S_1$  and  $S_2$  are both turned ON. All of the diodes are reverse-biased. Magnetizing inductors  $L_{m1}$  and  $L_{m2}$  as well as leakage inductors  $L_{k1}$  and  $L_{k2}$  are linearly charged by the input voltage source  $V_{in}$ .

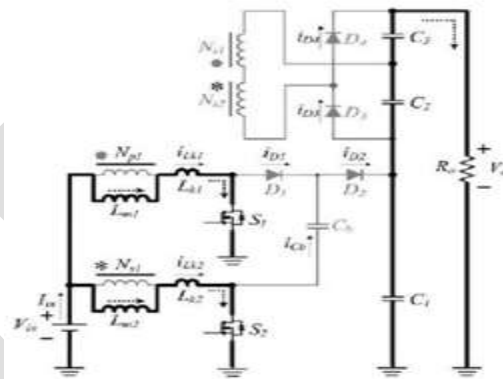


**Figure 5(a): Mode 1**

**Mode 2** [ $t_1, t_2$ ]: At  $t = t_1$ , the power switches  $S_2$  is switched OFF, thereby turned ON diodes  $D_2$  and  $D_4$ . The energy that magnetizing inductor  $L_{m2}$  has stored is transferred to the secondary side charging the output filter capacitor  $C_3$ . The input voltage source, magnetizing inductor  $L_{m2}$ , leakage inductor  $L_{k2}$ , and voltage-lift capacitor  $C_b$  release energy to the output filter capacitor  $C_1$  via diode  $D_2$ , thereby extending the voltage on  $C_1$ .

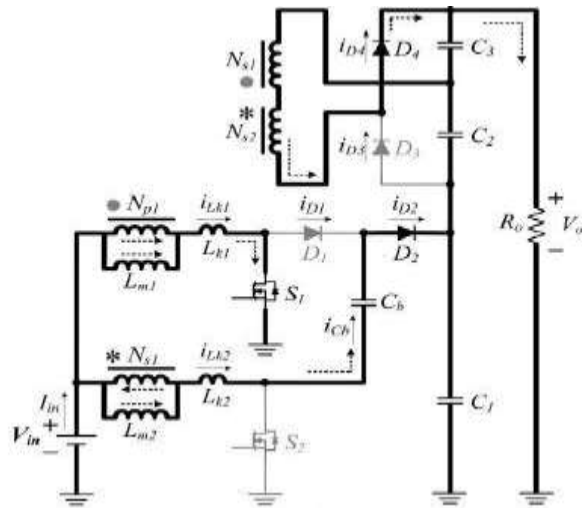


Figure 5(b): Mode 2

**Mode 3** [ $t_2, t_3$ ]: At  $t = t_2$ , diode  $D_2$  automatically switches OFF because the total energy of leakage inductor  $L_{k2}$  has been completely released to the output filter capacitor  $C_1$ . Magnetizing inductor  $L_{m2}$  transfers energy to the secondary side charging the output filter capacitor  $C_3$  via diode  $D_4$  until  $t_3$ .

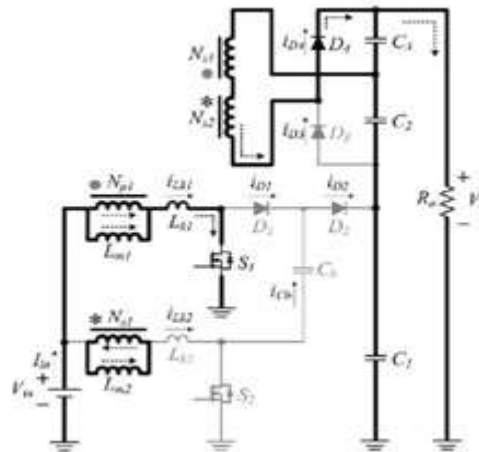


Figure 5(c): Mode 3

**Mode 4** [ $t_3, t_4$ ]: At  $t = t_3$ , the power switch  $S_2$  is switched ON and all the diodes are turned OFF. The operating states of modes 1 and 4 are similar.

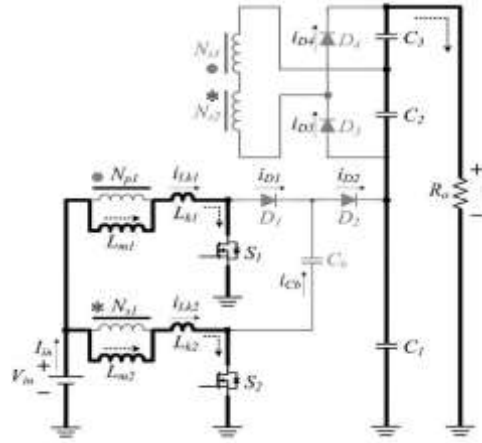


Figure 5(d): Mode 4

**Mode 5** [ $t_4, t_5$ ]: At  $t = t_4$ , the power switch  $S_1$  is switched OFF which turns ON diodes  $D_1$  and  $D_3$ . The energy stored in magnetizing inductor  $L_{m1}$  is transferred to secondary side charging the output filter capacitor  $C_2$ . The input voltage source and magnetizing inductor  $L_{m1}$  release energy to voltage-lift capacitor  $C_b$  via diode  $D_1$ , which stores extra energy in  $C_b$ .

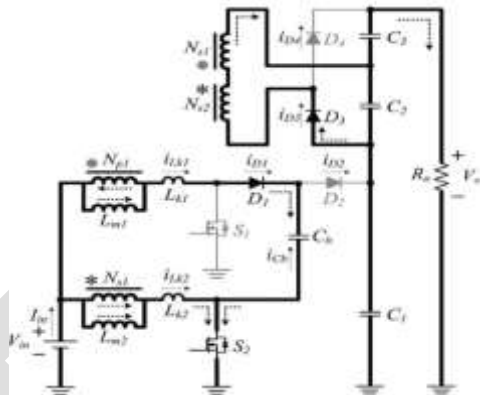


Figure 5(e): Mode 5

**Mode 6** [ $t_5, t_0$ ]: At  $t = t_5$ , diode  $D_1$  is automatically turned OFF because the total energy of leakage inductor  $L_{k1}$  has been completely released to voltage-lift capacitor  $C_b$ . Magnetizing inductor  $L_{m1}$  transfers energy to the secondary side charging the output filter capacitor  $C_2$  via diode  $D_3$  until  $t_0$ .

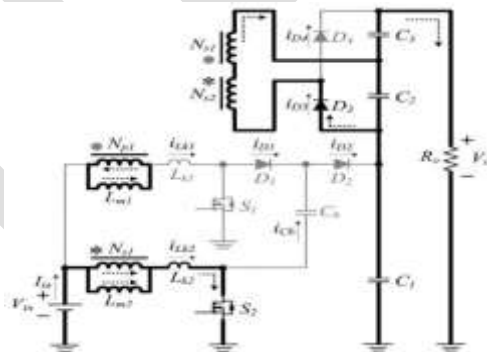


Figure 5(f): Mode 6

#### IV. STEADY STATE ANALYSIS

The transient characteristics of circuitry are disregarded to simplify the circuit performance analysis of the proposed converter in CCM, and some formulated assumptions are as follows:

- 1) All of the components in the proposed converter are ideal;
- 2) Leakage inductors  $L_{k1}$  and  $L_{k2}$  are neglected.
- 3) Voltage  $V_{cb}$ ,  $V_{c1}$ ,  $V_{c2}$ , and  $V_{c3}$  are considered to be constant because of infinitely large capacitance.

#### A. Voltage Gain

The first-phase converter can be regarded as a conventional boost converter, thus voltage  $V_{cb}$  can be derived from:

$$V_{cb} = V_{in} \frac{1}{1-D} \text{ ----- (1)}$$

When switch  $S_1$  is turned ON and switch  $S_2$  is turned OFF, voltage  $V_{c1}$  can be derived from:

$$V_{c1} = \frac{1}{1-D} V_{in} + V_{cb} = \frac{2}{1-D} V_{in} \text{ ----- (2)}$$

The output filter capacitors  $C_2$  and  $C_3$  are charged by energy transformation from the primary side. When  $S_2$  is in turn-on state and  $S_1$  is in turn-off state,  $V_{c2}$  is equal to induced voltage of  $N_{s1}$  plus induced voltage of  $N_{s2}$ , and when  $S_1$  is in turn-on state and  $S_2$  is in turn-off state,  $V_{c3}$  is also equal to induced voltage of  $N_{s1}$  plus induced voltage of  $N_{s2}$ . Thus, voltages  $V_{c2}$  and  $V_{c3}$  can be derived from

$$V_{c2} = V_{c3} = nV_{in} \left(1 + \frac{D}{1-D}\right) = \frac{n}{1-D} V_{in} \text{ ----- (3)}$$

The output voltage can be derived from:

$$V_o = V_{c1} + V_{c2} + V_{c3} = \frac{2n+2}{1-D} V_{in} \text{ ----- (4)}$$

The voltage gain of the proposed converter is

$$\frac{V_o}{V_{in}} = \frac{2n+2}{1-D} \text{ ----- (5)}$$

Above equation confirms that the proposed converter has a high step-up voltage gain without an extreme duty cycle.

#### B. Voltage Stresses on Semi Conductor Components

The voltage ripples on the capacitors are ignored to simplify the voltage stress analyses of the components of the proposed converter.

The voltage stresses on power switches  $S_1$  and  $S_2$  are derived from:

$$V_{s1} = V_{s2} = \frac{1}{1-D} V_{in} \text{ ----- (6)}$$

The voltage stresses on power switches  $S_1$  and  $S_2$  related to the output voltage  $V_o$  and the turns ratio  $n$  can be expressed as:

$$V_{s1} = V_{s2} = V_o - \frac{2n+1}{1-D} V_{in} \text{ ----- (7)}$$

The voltage stresses on the power switches account for half of output voltage  $V_o$ , even if turns ratio  $n$  is 0. The voltage stress on  $D_1$  is equal to  $V_{c1}$ , and the voltage stress on diode  $D_2$  is voltage  $V_{c1} - V_{cb}$ . These voltage stresses can be derived from:

$$V_{D1} = V_{c1} = \frac{2}{1-D} V_{in} \text{ ----- (8)}$$

$$V_{D2} = V_{c1} - V_{cb} = \frac{1}{1-D} V_{in} \text{ ----- (9)}$$

The voltage stressed on the diodes  $D_1$  and  $D_2$  and  $D_3$  and  $D_4$  related to the output voltage  $V_o$  and the turns ratio  $n$  can be expressed as:

$$V_{D1} = V_o - \frac{2n}{1-D} V_{in} \text{ ----- (10)}$$

$$V_{D3} = V_{D4} = V_o - \frac{2}{1-D} V_{in} \text{ ----- (12)}$$

$$V_{D2} = V_o - V_{in} = \frac{2}{1-D} V_{in} \text{ ----- (11)}$$

## V. MATLAB SIMULATION DIAGRAM

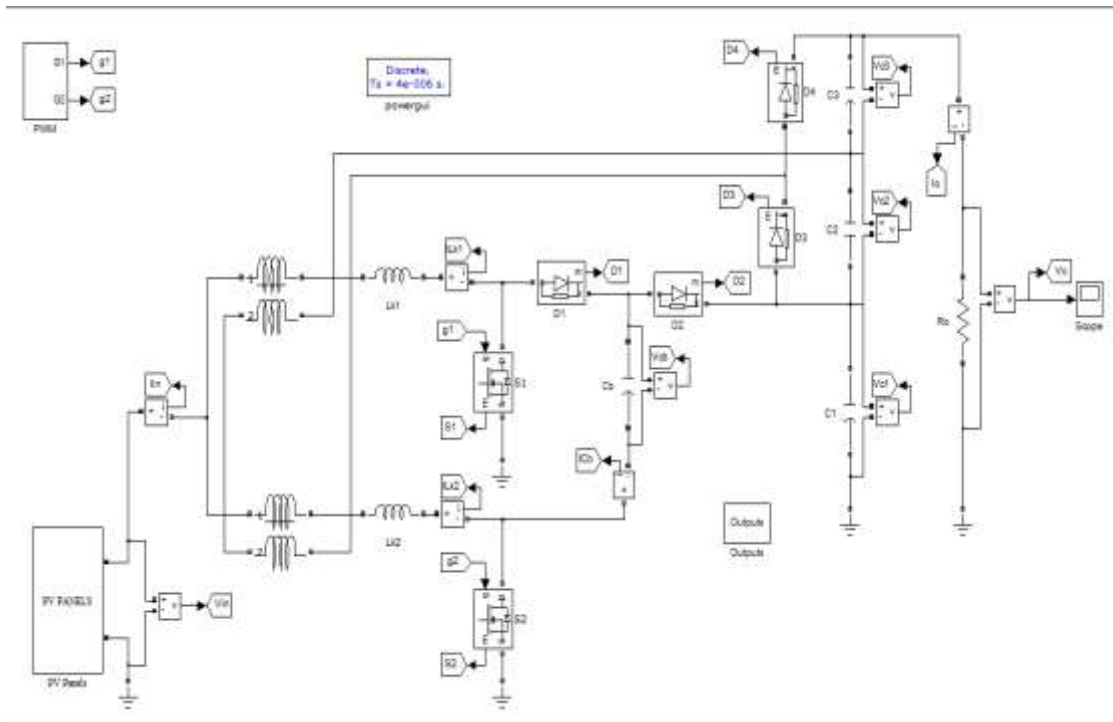


Figure 6: Simulation Diagram

## VI. MEASURED WAVEFORMS

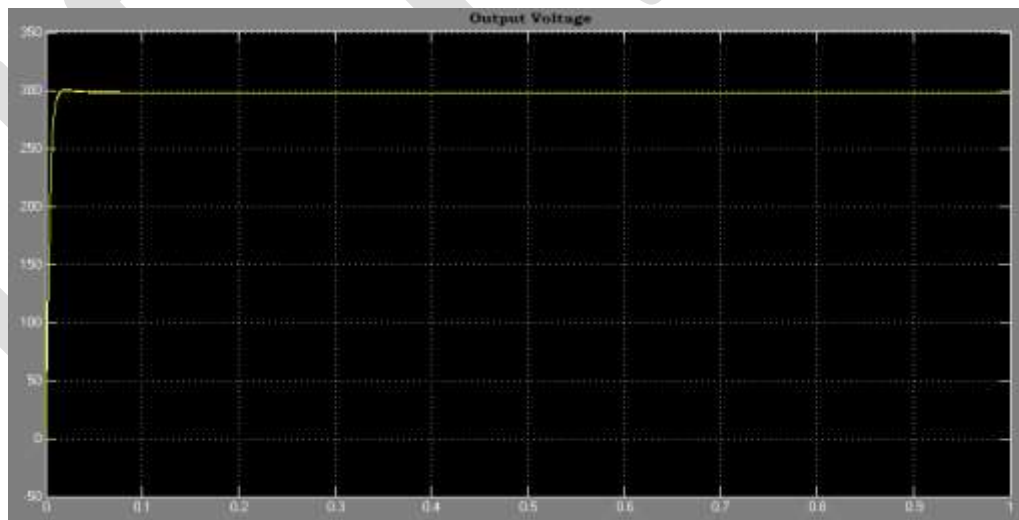


Figure 7(a): output voltage

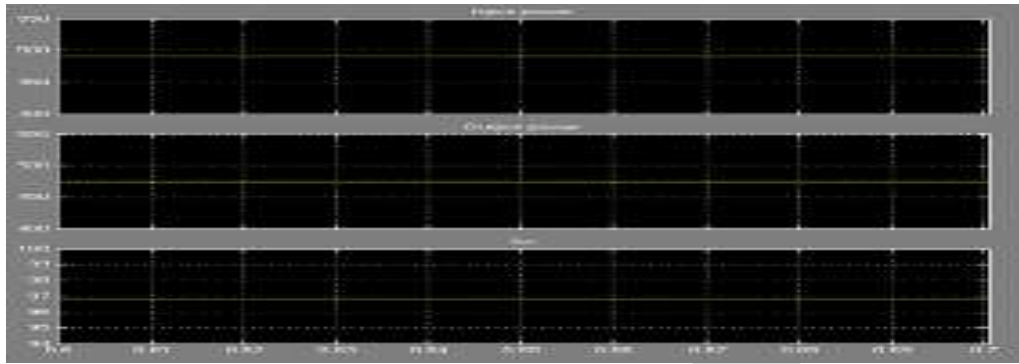


Figure 7(b): input and output power and efficiency

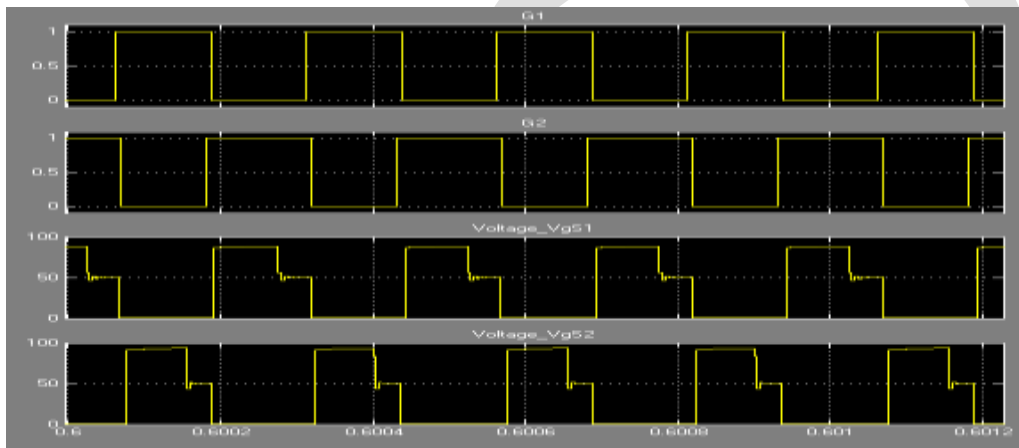


Figure 7(c): Measured  $V_{g1}$  and  $V_{g2}$  waveforms

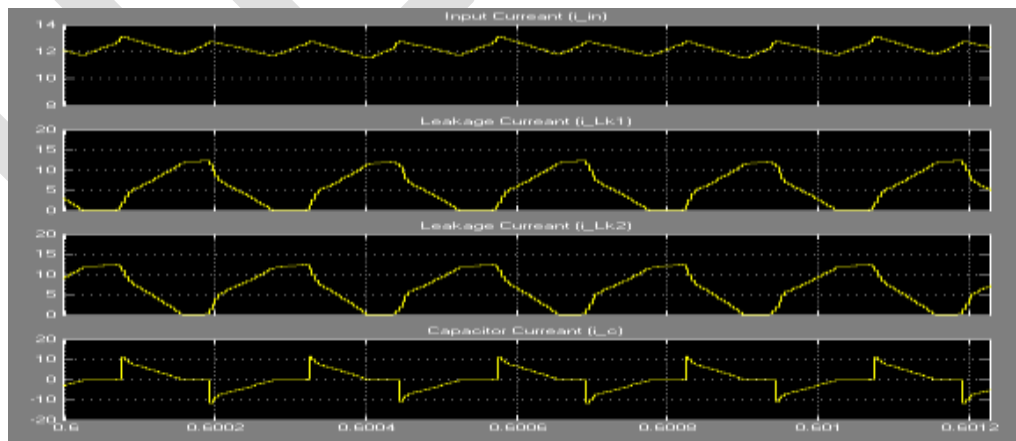


Figure 7(d): measured current wave forms

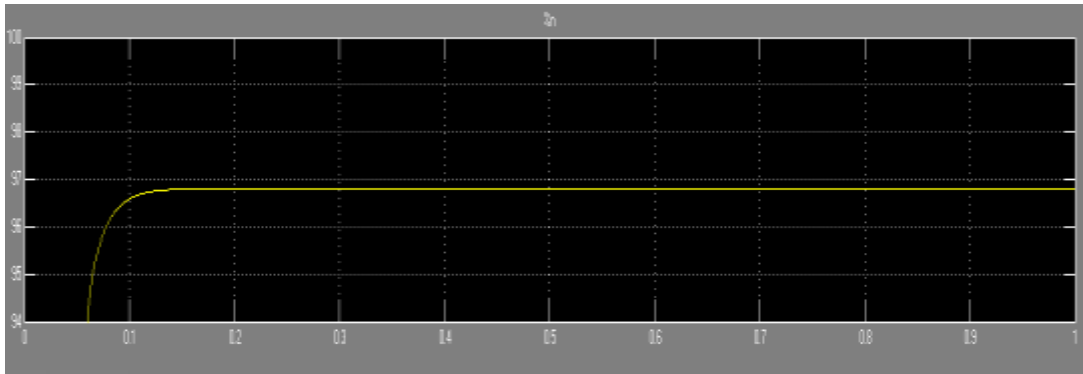


Figure 7(e): Measured output efficiency

## VII. PROPOSED CONCEPT

The proposed high step-up interleaved converter with a voltage multiplier module is shown in Figure 2. The voltage multiplier module is composed of two coupled inductors and two switched capacitors and is inserted between a conventional interleaved boost converter to form a modified boost-flyback-forward interleaved structure. When the switches turn off by turn, the phase whose switch is in OFF state performs as a flyback converter, and the other phase whose switch is in ON state performs as a forward converter.

Primary windings of the coupled inductors with  $N_p$  turns are employed to decrease input current ripple, and secondary windings of the coupled inductors with  $N_s$  turns are connected in series to extend voltage gain. The turn ratios of the coupled inductors are the same. The coupling references of the inductors are denoted by “.” and “\*”.

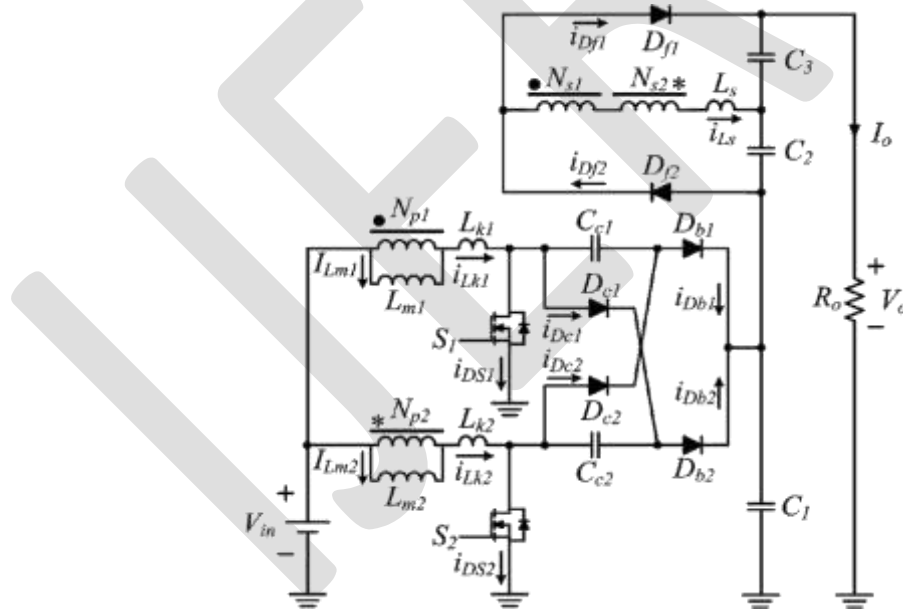


Figure 8: Equivalent Circuit of the Proposed Converter

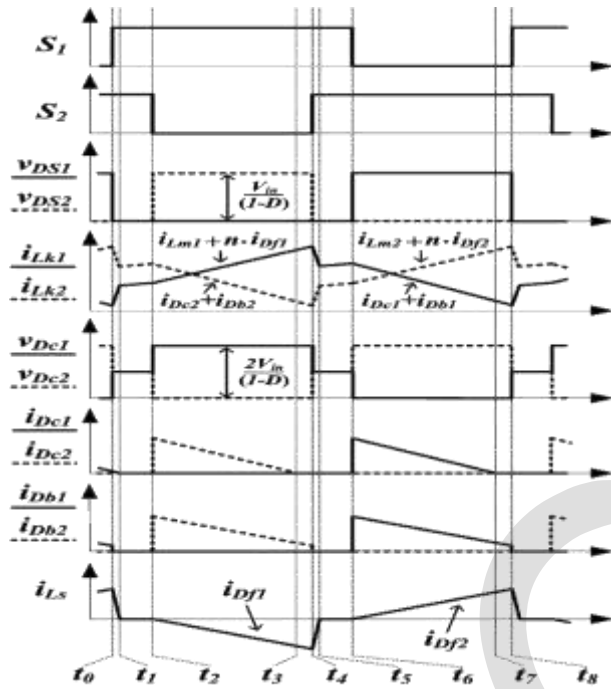


Figure 9: Steady Waveform of the Proposed Converter in CCM

### VIII. PROPOSED STEADY-STATE ANALYSIS

The transient characteristics of circuitry are disregarded to simplify the circuit performance analysis of the proposed converter in CCM, and some formulated assumptions are as follows:

- 1) All of the components in the proposed converter are ideal.
- 2) Leakage inductors  $L_{k1}, L_{k2}$ , and  $L_s$  are neglected.
- 3) Voltages on all capacitors are considered to be constant because of infinitely large capacitance.
- 4) Due to the completely symmetrical interleaved structure, the related components are defined as the corresponding symbols such as  $D_{c1}$  and  $D_{c2}$  defined as  $DC$ .

#### A. Step-up Gain

The voltage on clamp capacitor  $C_c$  can be regarded as an output voltage of the boost converter; thus, voltage  $V_{cc}$  can be derived from the equation.

$$V_{cc} = \frac{1}{1-D} V_{in} \text{----- (1)}$$

When one of the switches turns off, voltage  $V_{c1}$  can obtain a double output voltage of the boost converter derived from the equation.

$$V_{c1} = \frac{1}{1-D} V_{in} + V_{cc} = \frac{2}{1-D} V_{in} \text{----- (2)}$$

The output filter capacitors  $C_2$  and  $C_3$  are charged by energy transformation from the primary side. When  $S_2$  is in ON state and  $S_1$  is in OFF state,  $V_{c2}$  is equal to the sum of the induced voltage of  $N_{S1}$  and the induced voltage of  $N_{S2}$ , and when  $S_1$  is in ON state and  $S_2$  is in OFF state,  $V_{c3}$  is also equal to the sum of the induced voltage of  $N_{S1}$  and the induced voltage of  $N_{S2}$ . Thus, voltages  $V_{c2}$  and  $V_{c3}$  can be derived from:

$$V_{c2} = V_{c3} = nV_{in} \left( 1 + \frac{D}{1-D} \right) = \frac{n}{1-D} V_{in} \text{----- (3)}$$

The output voltage can be derived from:

$$V_o = V_{c1} + V_{c2} + V_{c3} = \frac{2n+2}{1-D} V_{in} \text{----- (4)}$$

In addition, the voltage gain of the proposed converter is

$$\frac{V_o}{V_{in}} = \frac{2n+2}{1-D} \text{----- (5)}$$

**B. Voltage Stresses on Semi Conductor Components**

Voltage ripple on capacitor was ignored to simplify the voltage stress analysis of the components of the proposed converter. The voltage stress on power switch *S* was clamped and derived from

$$V_{s1} = V_{s2} = \frac{2}{1-D} V_{in} = \frac{1}{2n+2} V_o \text{ ----- (6)}$$

The voltage stress can be derived from

$$V_{dc1} = V_{dc2} = \frac{2}{1-D} V_{in} = \frac{1}{n+1} V_o \text{ ----- (7)}$$

**IX. DESIGN AND EXPERIMENT OF PROPOSED CONVERTER**

A 0.5 kW prototype of the proposed high step-up converter is tested. The electrical specifications are  $V_{in} = 40\text{ V}$ ,  $V_o = 300\text{ V}$  and  $f_s = 40\text{ kHz}$ . The major components have been chosen as follows: Magnetizing inductors  $L_{m1}$  and  $L_{m2} = 133\mu\text{H}$ ; turn ratio  $n = 1$ ; power switches  $S_1$  and  $S_2$  are IRFP4227; diodes  $D_{c1}$  and  $D_{c2}$  are BYQ28E-200; diodes  $D_{b1}, D_{b2}, D_{f1}$  and  $D_{f2}$  are FCF06A-40; capacitors  $C_{c1}, C_{c2}, C_2$  and  $C_3 = 220\mu\text{F}$ ; and  $C_1 = 470\text{Mf}$ .

*Design Parameters*

PARAMETER	VALUE
Input Voltage	40 V DC
Output Voltage	380 V DC
Switching Frequency	40 KHz
Magnetizing Inductors ( $L_{m1}$ & $L_{m2}$ )	133 $\mu\text{H}$
Capacitors ( $C_{c1}, C_{c2}, C_2$ & $C_3$ )	220 $\mu\text{F}$
Capacitor ( $C_1$ )	470 $\mu\text{F}$
Output Power	500 W

The design consideration of the proposed converter includes component selection and coupled inductor design, which are based on the analysis present in the previous section. In the proposed converter, the values of primary leakage inductor of coupled inductors set as close as possible for current sharing performance and the leakage inductors  $L_{k1}$  and  $L_{k2}$  are  $1.6\mu\text{H}$ . Due to the performance of high step-up gain, the turn ratio  $n$  can be set as one for the prototype circuit with 40 V input voltage and 380 V output voltage to reduce cost, volume and conduction loss of winding. Thus, copper resistance which affect efficiency much can be decreased.

**X. MATLAB SIMULATION DIAGRAM**

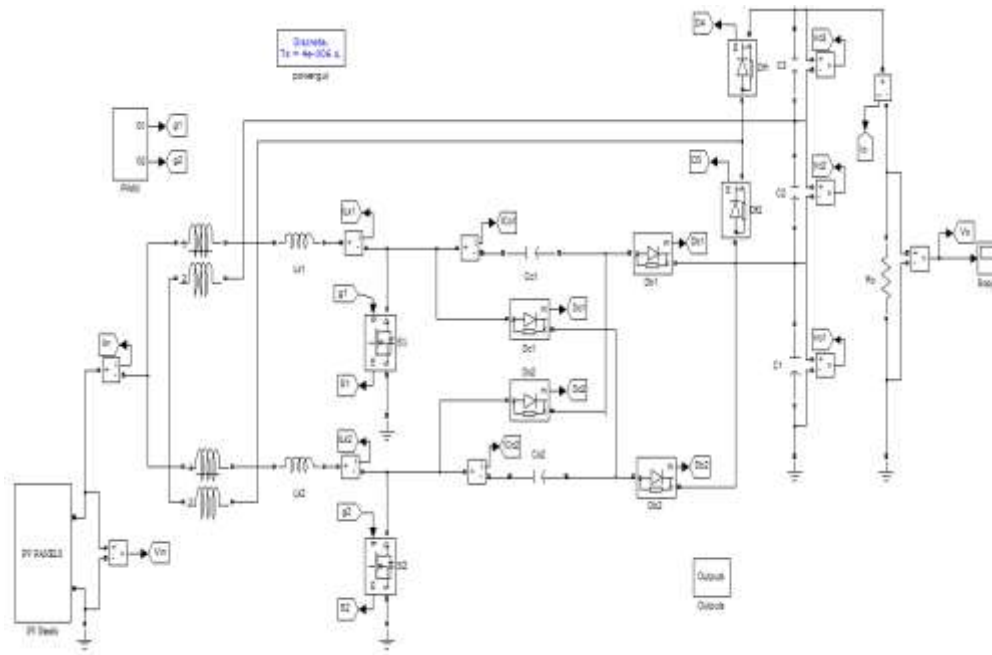


Figure 10: Simulation diagram

## XI. MEASURED WAVEFORMS

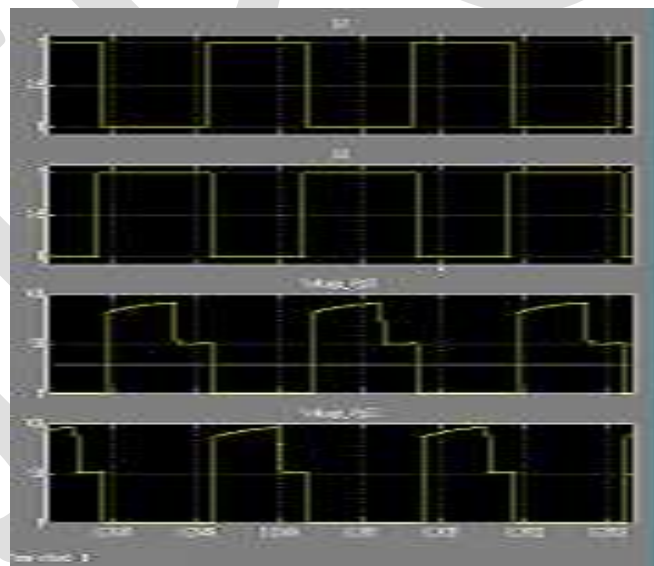


Figure 11(a): gate pulse and  $V_{gs1}$  and  $V_{gs2}$  measured wave forms

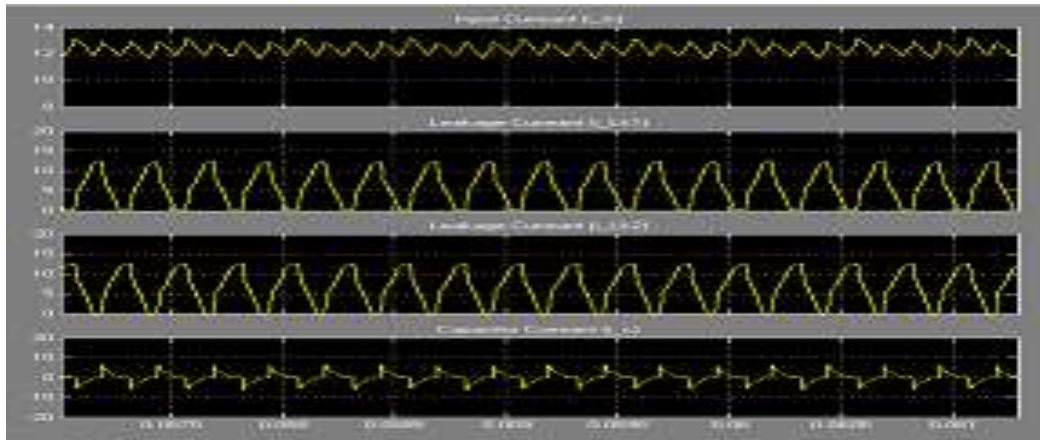


Figure 11(b): Measured current wave forms

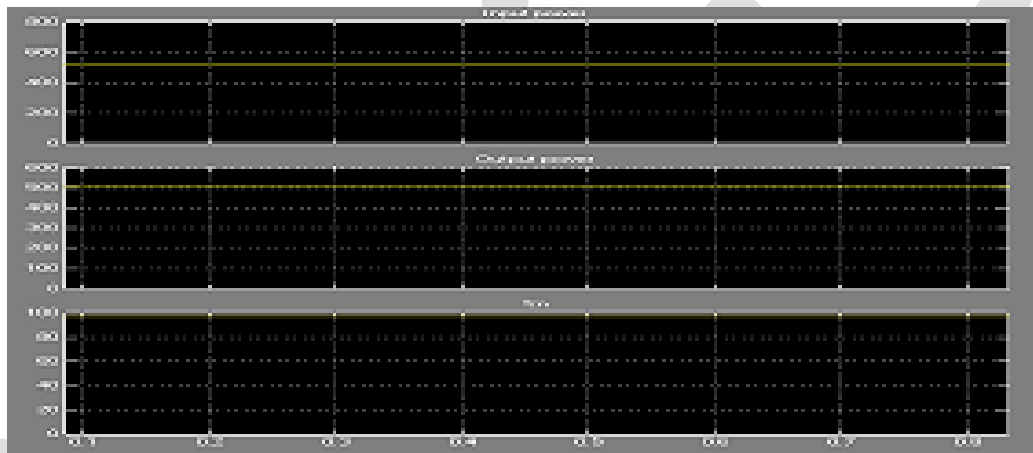


Figure 11(c): input and output power and efficiency waveforms

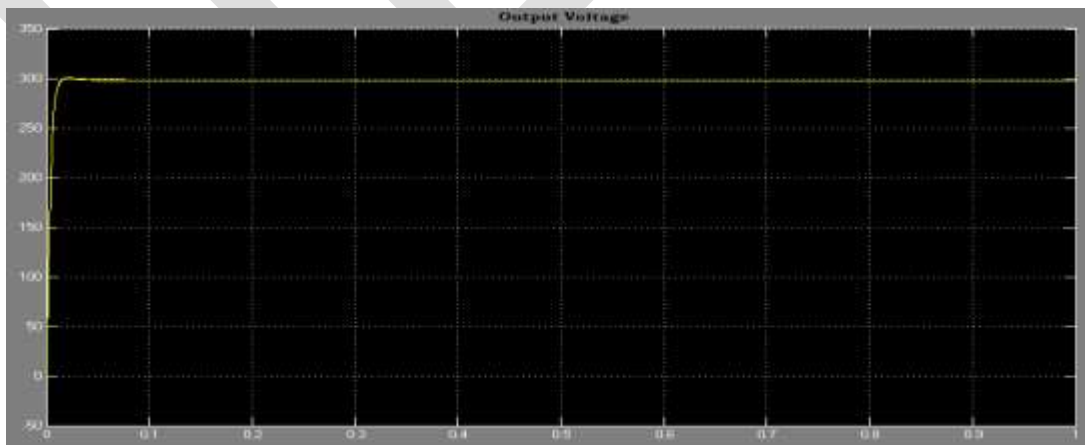


Figure 11(d): Measured output voltage

## XII. CONCLUSION

This paper has presented the theoretical analysis of steady state, related consideration, simulation results for the proposed converter. The proposed converter has successfully implemented an efficient high step-up conversion through the voltage multiplier module. The interleaved structure reduces the input current ripple and distributes the current through each component. In addition, the lossless passive clamp function recycles the leakage energy and constrains a large voltage spike across the power switch. Meanwhile, the voltage stress on the power switch is restricted and much lower than the output voltage (300 V). Furthermore, the full-load efficiency is 96.4% at  $P_o = 500 W$ , and the highest efficiency is 97.7%. Thus, the proposed converter is suitable for high-power or renewable energy applications that need high step-up conversion.

## REFERENCES:

- [1] C. Evangelista, P. Puleston, F. Valenciaga, and L.M. Fridman, "Lyapunov designed super-twisting sliding mode control for wind energy conversion optimization," *IEEE Trans. Ind. Electron.*, vol. 60, no. 2, pp. 538–545, Feb. 2013.
- [2] T. Kefalas and A. Kladas, "Analysis of transformers working under heavily saturated conditions in grid-connected renewable energy systems," *IEEE Trans. Ind. Electron.*, vol. 59, no. 5, pp. 2342–2350, May 2012.
- [3] Y. Xiong, X. Cheng, Z. J. Shen, C. Mi, H. Wu, and V. K. Garg, "Prognostic and warning system for power-electronic modules in electric, hybridelectric, and fuel-cell vehicles," *IEEE Trans. Ind. Electron.*, vol. 55, no. 6, pp. 2268–2276, Jun. 2008.
- [4] A. K. Rathore, A. K. S. Bhat, and R. Oruganti, "Analysis, design and experimental results of wide range ZVS active-clamped L–L type currentfed DC/DC converter for fuel cells to utility interface," *IEEE Trans. Ind. Electron.*, vol. 59, no. 1, pp. 473–485, Jan. 2012.
- [5] C. T. Pan and C. M. Lai, "A high-efficiency high step-up converter with low switch voltage stress for fuel-cell system applications," *IEEE Trans. Ind. Electron.*, vol. 57, no. 6, pp. 1998–2006, Jun. 2010.
- [6] R. J. Wai and R. Y. Duan, "High step-up converter with coupled-inductor," *IEEE Trans. Power Electron.*, vol. 20, no. 5, pp. 1025–1035, Sep. 2005.
- [7] S. K. Changchien, T. J. Liang, J. F. Chen, and L. S. Yang, "Novel high step-up DC–DC converter for fuel cell energy conversion system," *IEEE Trans. Ind. Electron.*, vol. 57, No. 6, pp. 2007–2017, Jun. 2010.
- [8] Y. P. Hsieh, J. F. Chen, T. J. Liang, and L. S. Yang, "Novel high step-up DC–DC converter with coupled-inductor and switched-capacitor techniques for a sustainable energy system," *IEEE Trans. Power Electron.*, vol. 26, no. 12, pp. 3481–3490, Dec. 2011.
- [9] C. Hua, J. Lin, and C. Shen, "Implementation of a DSP-controlled photovoltaic system with peak power tracking," *IEEE Trans. Ind. Electron.*, vol. 45, no. 1, pp. 99–107, Feb. 1998.
- [10] J. M. Carrasco, L. G. Franquelo, J. T. Bialasiewicz, E. Galvan, R. C. P. Guisado, M. A. M Prats, J. I. Leon, and N. Moreno-Alfonso, "Power-electronic systems for the grid integration of renewable energy sources: A survey," *IEEE Trans. Ind. Electron.*, vol. 53, no. 4, pp. 1002–1016, Jun. 2006.
- [11] J. T. Bialasiewicz, "Renewable energy systems with photovoltaic power generators: Operation and modeling," *IEEE Trans. Ind. Electron.*, vol. 55, no. 7, pp. 2752–2758, Jul. 2008.
- [12] F. S. Pai, "An improved utility interface for micro-turbine generation system with stand-alone operation capabilities," *IEEE Trans. Ind. Electron.*, vol. 53, no. 5, pp. 1529–1537, Oct. 2006.